ABER of Dual Predetection EGC in Correlated Nakagami-m Fading Channels with Arbitrary m

Prabhat Patel, *Student Member, IEEE,* P. R. Sahu, *Member, IEEE,* and A. K. Chaturvedi, *Senior Member, IEEE*

***Abstract*—We have analyzed the performance of a predetection equal gain combining (EGC) receiver over correlated Nakagami-m fading channels with arbitrary and non-identical m and unequal branch SNRs. Closed-form expression for average bit error rate (ABER) for coherent binary modulation schemes is derived by finding the characteristic function (CHF) of the sum of two correlated Nakagami-m envelopes with different fading parameters and then using Parseval's theorem. The derived expression can be viewed as a generalization of four different special cases reported in the literature. It was observed that depending on the values of m_1 and m_2 the ABER curves for two different pairs of (m_1, m_2) may intersect. Thus, if the performance corresponding to a pair is inferior to another pair at any SNR, this may not hold true over the entire SNR range.**

***Index Terms*—ABER, predetection EGC, Nakagami-*m* fading.**

I. INTRODUCTION

PERFORMANCE analysis of diversity combining schemes over Nakagami-m fading channels usually consider identical fading parameters for different branches. However, in practice, since the channels corresponding to the different branches of a combiner can have different physical characteristics [1], the fading parameters need not be identical. In fact, a field measurement report states that the fading parameter of a Nakagami-m channel depends on the surface irregularities and the strength of the line-of-sight signal component and can vary widely (typically 1-15) [2].

To address this issue maximal ratio combining (MRC) scheme over correlated Nakagami-m channels with the branches having different fading parameters has been analyzed in [1]. In this letter, we investigate the average bit error rate (ABER) performance of a dual-diversity equal gain combining (EGC) receiver in correlated Nakagami-m channels with arbitrary and non-identical m for coherent binary modulation schemes. The average SNRs are allowed to be non-identical in both the branches.

Performance study of dual-diversity predetection EGC receiver has been done for a number of cases [3]-[6]. Closed-form solutions for the ABER of the EGC with two or three branches operating over a Rayleigh channel has been obtained in [3]. This work was generalized in [4] where the performance of a dual-diversity EGC receiver has been studied for independent Nakagami-m channels and non-identical m. For a correlated Rayleigh channel the ABER performance has been studied for coherent binary modulation schemes in [5]. This was generalized in [6] where ABER for correlated Nakagami-m channels with identical m has been obtained for some coherent and non-coherent modulation schemes.

The paper is organized as follows. In Section II we discuss the system and channel models. In Section III we present the derivation of expressions for ABER for coherent binary modulation schemes. Numerical and simulation results have been presented in Section IV. Finally, in Section V we conclude the paper.

Manuscript received March 13, 2008. The associate editor coordinating the review of this letter and approving it for publication was P. Cotae.

P. Patel and A. K. Chaturvedi are with the Department of Electrical Engineering, Indian Institute of Technology Kanpur, India (e-mail: {ppatel, akc} @iitk.ac.in).

P. R. Sahu is with the Department of ECE, Indian Institute of Technology Guwahati, India (e-mail: prs@iitg.ernet.in).

Digital Object Identifier 10.1109/LCOMM.2008.080406.

II. SYSTEM AND CHANNEL MODEL

We consider a dual-diversity EGC receiver. Each branch of the receiver receives faded signal corrupted by additive white Gaussian noise (AWGN). The channel fading is assumed to be slow and having Nakagami-m statistics.

The instantaneous SNR at the dual-EGC combiner output is $\gamma = \alpha^2$, where α is given by [7]

$$\alpha = \sqrt{\frac{E_b}{2N_0}}(\alpha_1 + \alpha_2), \tag{1}$$

where α_1 and α_2 are the instantaneous amplitudes, E_b is the energy per transmitted bit and N_0 is the AWGN power spectral density. The amplitudes α_1 and α_2 are correlated Nakagami-m distributed random variables with arbitrary fading parameters m_1 and m_2 respectively and joint probability density function [8]

$$f_{\alpha_1,\alpha_2}(\alpha_1,\alpha_2) = 4(1-\rho)^{m_2} \sum_{k=0}^{\infty} \frac{(m_1)_k \rho^k}{k!} \left(\frac{m_1}{\Omega_1(1-\rho)}\right)^{m_1+k}$$
$$\times \frac{\alpha_1^{2m_1+2k-1} e^{\frac{-m_1\alpha_1^2}{\Omega_1(1-\rho)}}}{\Gamma(m_1+k)} \left(\frac{m_2}{\Omega_2(1-\rho)}\right)^{m_2+k} \frac{\alpha_2^{2m_2+2k-1} e^{\frac{-m_2\alpha_2^2}{\Omega_2(1-\rho)}}}{\Gamma(m_2+k)}$$
$$\times {}_1F_1\left(m_2 - m_1; m_2+k; \frac{m_2\rho}{\Omega_2(1-\rho)}\alpha_2^2\right), \tag{2}$$

where $\Omega_i = \mathrm{E}\left[\alpha_i^2\right], i = 1, 2$ denotes the average signal power, $\Gamma(\cdot)$ is the Gamma function, $(\cdot)_k$ is the Pochhammer's symbol, and ρ is the power correlation coefficient defined as

$$\rho = \frac{cov(\alpha_1^2, \alpha_2^2)}{\sqrt{var(\alpha_1^2)var(\alpha_2^2)}}, \ 0 \le \rho < 1. \tag{3}$$

III. ABER PERFORMANCE

A general expression for the ABER of an EGC receiver for coherent modulation schemes is given by [4]

$$P_s = \frac{1}{2} - \frac{1}{2\pi}\int_0^{\infty} t^{-1} e^{-t} \Im\{\Phi_\alpha(2\sqrt{at})\}dt, \tag{4}$$

where $\Phi_\alpha(\cdot)$ is the characteristic function (CHF) of α defined in (1), $\Im\{\cdot\}$ denotes the imaginary part and the parameter a is 1 and 0.5 for BPSK and BFSK modulations, respectively.

In order to find $\Phi_\alpha(s)$ we first find $\Phi_{\alpha_1+\alpha_2}(s)$. An expression for $\Phi_{\alpha_1+\alpha_2}(s)$ can be obtained from (2) by using the definition of the characteristic function and using Eqs. 3.462.1, 8.335.1 and 9.240 of [9]. Now using (1) and denoting average SNR of the ith branch by

$$\bar{\gamma_i} = \Omega_i(E_s/N_0) \quad (5)$$

$\Phi_\alpha(s)$ can be written as

$$\Phi_\alpha(s) = (1-\rho)^{m_2}\sum_{k=0}^{\infty}\frac{(m_1)_k}{k!}\rho^k\left(A(\overline{\gamma_1};s)+jB(\overline{\gamma_1};s)\right) \times\left\{\sum_{n=0}^{\infty}\frac{(m_2-m_1)_n\rho^n}{n!}\left(A(\overline{\gamma_2};s)+jB(\overline{\gamma_2};s)\right)\right\}, \quad (6)$$

where

$$\begin{aligned}
A(\overline{\gamma_1};s) &= {}_1F_1\left(m_1+k;\frac{1}{2};\frac{-s^2\overline{\gamma_1}(1-\rho)}{8m_1}\right),\\
B(\overline{\gamma_1};s) &= \frac{s\sqrt{\overline{\gamma_1}(1-\rho)}\Gamma(m_1+k+1/2)}{\sqrt{2m_1}\Gamma(m_1+k)}\\
&\quad\times{}_1F_1\left(m_1+k+1/2;\frac{3}{2};\frac{-s^2\overline{\gamma_1}(1-\rho)}{8m_1}\right),\\
A(\overline{\gamma_2};s) &= {}_1F_1\left(m_2+k+n;\frac{1}{2};\frac{-s^2\overline{\gamma_2}(1-\rho)}{8m_2}\right),\\
B(\overline{\gamma_2};s) &= \frac{s\sqrt{\overline{\gamma_2}(1-\rho)}\Gamma(m_2+k+n+1/2)}{\sqrt{2m_2}\Gamma(m_2+k+n)}\\
&\quad\times{}_1F_1\left(m_2+k+n+1/2;\frac{3}{2};\frac{-s^2\overline{\gamma_2}(1-\rho)}{8m_2}\right).
\end{aligned}$$

By algebraic manipulations in (6) and using Eq. 9.212.1 of [9] an expression for $\Im\{\Phi_\alpha(2\sqrt{at})\}$ is given in (7) where

$$c_1 = \frac{a(1-\rho)}{2m_1}$$

and

$$c_2 = \frac{a(1-\rho)}{2m_2}.$$

Substituting (7) in (4) and solving the integrals in the resulting equation using Eq. C.1 of [4], which we reproduce below for convenience

$$\begin{aligned}
&\int_0^\infty x^{(\nu-1)}e^{-bx}\prod_{k=1}^{n}{}_1F_1(a_k;b_k;c_kx)dx\\
&= b^{-\nu}\Gamma(\nu)F_A\left(\nu;a_1,\cdots,a_n;b_1,\cdots,b_n;\frac{c_1}{b},\cdots,\frac{c_n}{b}\right)\\
&\left[b_k>0,\nu>0,\sum c_k<b\right],
\end{aligned}$$

we obtain the expression for ABER given in (8) where $F_2(\cdot;\cdot,\cdot,\ldots;\cdot,\cdot,\ldots;\cdot,\cdot,\ldots)$ denotes the hypergeometric function of two variables [9].

It is worthwhile to point out that (8) is a generalization of some earlier reported expressions. Thus, for $m_1 = m_2 = m$ it reduces to Eq. 21 of [6]. It may be noted that Eq. 21 of [6] itself was a generalization of Eq. 29 of [4] for $\rho = 0$ and $m_1 = m_2 = m$. We have verified that, as expected, (8) gives the same result for $m_1 = m_2 = 1$ as Eq. 15 of [5], even though it does not reduce to that expression. This is because [5] uses Hermite polynomials to represent ${}_1F_1(\cdot;\cdot;\cdot)$. Again, as pointed out in [5], it may be noted that for $\rho = 0$, Eq. 15 of [5] reduces to Eq. 23 of [3]. Thus we can say that the results of [3], [4], [5] and [6] can be viewed as special cases of our result.

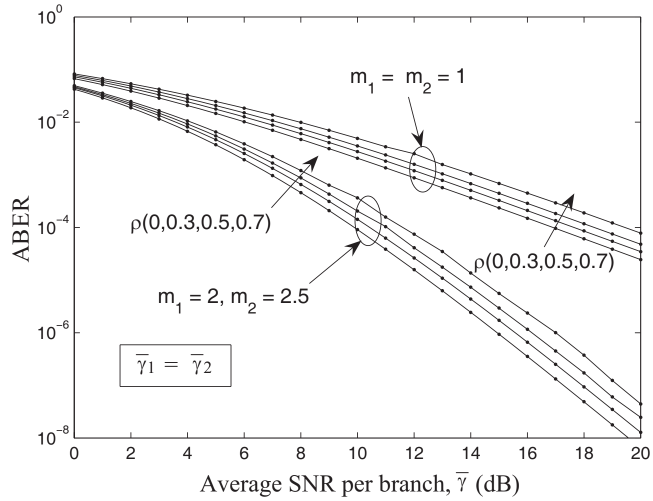

Fig. 1. ABER for different values of ρ for two pairs of (m_1, m_2) given by (1, 1) and (2, 2.5).

IV. Numerical and Simulation Results

In this section the ABER versus average SNR per branch $\bar{\gamma} \triangleq (\bar{\gamma}_1 + \bar{\gamma}_2)/2$ has been plotted for three different cases. In all the cases the ABER expression (8) has been evaluated for BPSK modulation. The markers shown in Fig. 1 show the simulation results.

In Fig. 1 the ABER has been plotted for two pairs of (m_1, m_2) for four different values of ρ given by 0, 0.3, 0.5 and 0.7. From the figure it can be seen that, as expected, ABER degrades with increase in ρ and improves for higher values of m. The curves obtained from (21) of [6] for identical m in the two branches have been found to be matching with the curves obtained from (8) for the same case. Furthermore, unbalance in the input average SNRs was found to degrade the ABER performance.

It may be noted that for any two pairs of (m_1, m_2) the ABER curves have different slopes. Thus, intuitively, if we consider a pair (m_1, m_2) and another pair $(m_1 - \delta, m_2 + \lambda)$ where $\delta, \lambda > 0$ i.e. we decrease the fading in one branch and increase in the other branch, then there is a possibility of intersection in the ABER curves for these two pairs. Keeping this in view we explored for pairs with intersecting ABER curves. In Fig. 2 ABER curves for two pairs of (m_1, m_2) given by $(1, 4)$ and $(0.5, 6)$ have been shown. It can be seen that the crossover point of the two curves is around 17 dB of average SNR per branch. In the same figure we have also plotted the curves for MRC for the same pairs of (m_1, m_2). The MRC curves have been plotted by using the expression for ABER given in [10]. The crossover point for MRC turns out to be 9 dB which is significantly lower than 17 dB, the crossover point for EGC.

$$\begin{aligned}\Im\{\Phi_\alpha(2\sqrt{at})\} &= (1-\rho)^{m_2+\frac{1}{2}}\sum_{k=0}^{\infty}\frac{(m_1)_k\rho^k}{k!}\sum_{n=0}^{\infty}\frac{(m_2-m_1)_n\rho^n\sqrt{2a}}{n!}\\ &\times\Bigg(\frac{\sqrt{\overline{\gamma_2}}\Gamma(m_2+k+n+1/2)}{\sqrt{m_2}\Gamma(m_2+k+n)}\sqrt{t}e^{-(c_1\overline{\gamma_1}+c_2\overline{\gamma_2})t}\ {}_1F_1\left(\frac{1}{2}-m_1-k;\frac{1}{2};c_1\overline{\gamma_1}t\right)\ {}_1F_1\left(1-m_2-k-n;\frac{3}{2};c_2\overline{\gamma_2}t\right)\\ &+\frac{\sqrt{\overline{\gamma_1}}\Gamma(m_1+k+1/2)}{\sqrt{m_1}\Gamma(m_1+k)}\sqrt{t}e^{-(c_1\overline{\gamma_1}+c_2\overline{\gamma_2})t}\ {}_1F_1\left(\frac{1}{2}-m_2-k-n;\frac{1}{2};c_2\overline{\gamma_2}t\right)\ {}_1F_1\left(1-m_1-k;\frac{3}{2};c_1\overline{\gamma_1}t\right)\Bigg)\end{aligned}\tag{7}$$

$$\begin{aligned}P_s &= \frac{1}{2}-\frac{\sqrt{a}(1-\rho)^{m_2+\frac{1}{2}}}{\sqrt{2\pi(c_1\overline{\gamma_1}+c_2\overline{\gamma_2}+1)}}\sum_{k=0}^{\infty}\frac{(m_1)_k\rho^k}{k!}\sum_{n=0}^{\infty}\frac{(m_2-m_1)_n\rho^n}{n!}\\ &\times\Bigg(\frac{\sqrt{\overline{\gamma_2}}\Gamma(m_2+k+n+1/2)}{\sqrt{m_2}\Gamma(m_2+k+n)}F_2\left(\frac{1}{2};\frac{1}{2}-m_1-k,1-m_2-k-n;\frac{1}{2},\frac{3}{2};\frac{c_1\overline{\gamma_1}}{c_1\overline{\gamma_1}+c_2\overline{\gamma_2}+1},\frac{c_2\overline{\gamma_2}}{c_1\overline{\gamma_1}+c_2\overline{\gamma_2}+1}\right)\\ &+\frac{\sqrt{\overline{\gamma_1}}\Gamma(m_1+k+1/2)}{\sqrt{m_1}\Gamma(m_1+k)}F_2\left(\frac{1}{2};\frac{1}{2}-m_2-k-n,1-m_1-k;\frac{1}{2},\frac{3}{2};\frac{c_2\overline{\gamma_2}}{c_1\overline{\gamma_1}+c_2\overline{\gamma_2}+1},\frac{c_1\overline{\gamma_1}}{c_1\overline{\gamma_1}+c_2\overline{\gamma_2}+1}\right)\Bigg)\end{aligned}\tag{8}$$

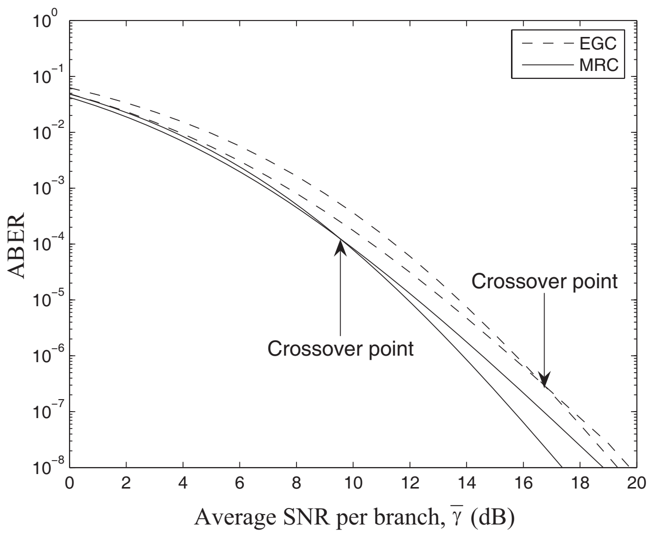

Fig. 2. ABER showing the crossover points for two pairs of (m_1, m_2) given by $(1, 4)$ and (0.5, 6) for MRC and EGC.

TABLE I
NUMBER OF TERMS OF (8) REQUIRED FOR SIXTH SIGNIFICANT DIGIT ACCURACY

SNR (dB)	ρ	$m_1 = 2, m_2 = 2.5$		$m_1 = 2, m_2 = 5$	
		N	BER	N	BER
5.0	0.3	14	0.004645	16	0.002740
	0.5	23	0.005474	28	0.003048
	0.7	50	0.006546	53	0.003412
10.0	0.3	12	0.000142	16	0.000031
	0.5	22	0.000205	25	0.000042
	0.7	45	0.000321	51	0.000058

In order to check the convergence of the ABER expression, some ABER values accurate till the sixth significant digit have been listed in Table I. The values of m_1 and m_2 have been taken to be different because for identical values of m_1 and m_2, (8) reduces to a single infinite series. For convenience, identical number of terms denoted as N, have been retained in the two infinite series. From the table it can be noted that the required number of terms increases with increase in ρ for a constant SNR, while it remains same or decreases with an increase in SNR when ρ is constant. Further, the number of terms required increases when the fading in one branch is kept constant while it is decreased in the other branch.

V. CONCLUSION

We have analyzed the performance of a predetection EGC receiver over correlated Nakagami-m fading channels with non-identical m and unequal branch SNRs. The derived expression can be viewed as a generalization of four different special cases reported in the literature. It was observed that depending on the values of m_1 and m_2, the ABER curves for two different pairs of (m_1, m_2) may intersect. Thus, if the performance corresponding to a pair is inferior to another pair at any SNR, this may not hold true over the entire SNR range.

REFERENCES

[1] Q. T. Zhang, "A generic correlated Nakagami fading model for wireless communications," *IEEE Trans. Commun.*, vol. 51, no. 11, pp. 1745–1748, Nov. 2003.

[2] W. R. Braun and U. Dersch, "A physical mobile radio channel model," *IEEE Trans. Veh. Technol.*, vol. 40, no. 2, pp. 472–482 May 1991.

[3] Q. T. Zhang, "Probability of error for equal-gain combiners over Rayleigh channels: some closed-form solutions," *IEEE Trans. Commun.*, vol. 45, pp. 270–273, Mar. 1997.

[4] A. Annamalai, C. Tellambura, and Vijay K. Bhargava, "Equal-gain diversity receiver performance in wireless channels," *IEEE Trans. Commun.*, vol. 48, no. 10, pp. 1732–1745, Oct. 2000.

[5] R. K. Mallik, M. Z. Win, and J. H. Winters, "Performance of dual-diversity predetection EGC in correlated Rayleigh fading with unequal branch SNRs," *IEEE Trans. Commun.*, vol. 50, no. 7, pp. 1041–1044, July 2002.

[6] G. K. Karagiannidis, D. A. Zogas, and S. A. Kotsopoulos, "BER performance of dual predetection EGC in correlative Nakagami-m fading," *IEEE Trans. Commun.*, vol. 52, no. 1, pp. 50–53, Jan. 2004.

[7] M. K. Simon and M. Alouini, *Digital Communication over Fading Channels*, 1st ed. New York: Wiley, 2000.

[8] J. Reig, L. Rubio, and N. Cardona, "Bivariate Nakagami-m distribution with arbitrary fading parameters," *IEE Electron. Lett.*, vol. 38, no. 25, pp. 1715–1717, Dec. 2002.

[9] I. S. Grashteyn and I. M. Ryzhik, *Table of Integrals, Series, and Products*, 4th ed. New York: Academic, 1980.

[10] V. A. Aalo, T. Piboongungon, and P. Efthymoglou, "Another look at the performance of MRC schemes in Nakagami-m fading channels with arbitrary parameters," *IEEE Trans. Commun.*, vol. 53, no. 12, pp 2002–2005, Dec. 2005.